

VUV photoluminescence properties of $Y_{1-x}Gd_xVO_4:Eu$ phosphors prepared by ultrasonic spray pyrolysis

K. Park*, S.W. Nam, M.H. Heo

Faculty of Nanotechnology and Advanced Materials Engineering, Sejong University, Seoul 143-747, Republic of Korea

Received 7 December 2009; received in revised form 5 January 2010; accepted 3 February 2010

Available online 9 March 2010

Abstract

The red-emitting $(Y_{1-x}Gd_x)_{0.94}Eu_{0.06}VO_4$ ($0 \leq x \leq 1.0$) phosphors were synthesized by ultrasonic spray pyrolysis. The $(Y_{1-x}Gd_x)_{0.94}Eu_{0.06}VO_4$ ($0 \leq x \leq 1.0$) phosphors had the tetragonal xenotime structure with a space group of $I4_1/amd$ ($1\ 4\ 1$). The calculated crystallite sizes of the annealed phosphors ranged from 58 to 68 nm. In this study, we discussed the photoluminescence properties of the $(Y_{1-x}Gd_x)_{0.94}Eu_{0.06}VO_4$ phosphors under VUV excitation, depending on Gd content. The emission intensity of the $(Y_{1-x}Gd_x)_{0.94}Eu_{0.06}VO_4$ phosphors increased with increasing Gd content up to $x = 0.5$, and then decreased with a further increase in Gd content. The purest red color was obtained for the $(Y_{0.5}Gd_{0.5})_{0.94}Eu_{0.06}VO_4$ phosphors.

© 2010 Elsevier Ltd and Techna Group S.r.l. All rights reserved.

Keywords: A. Powders; chemical preparation; B. X-ray methods; C. Optical properties

1. Introduction

Oxide phosphors have received considerable attention due to the need for new luminescent materials suitable for the display devices. In particular, rare-earth (R) vanadates, RVO_4 , have attracted interest as a laser medium and as a host material for rare-earth ions in luminescent displays [1,2]. They have either a xenotime (tetragonal) or monazite (monoclinic) structure at ordinary pressures. YVO_4 has been extensively used as a host for lanthanide ion because of high luminescence quantum yields for the f–f transitions [3]. Also, $GdVO_4$ has the $ZrSiO_4$ structure ($a = b = 7.2126$ Å and $c = 6.3483$ Å), belonging to the space group $I4_1/amd$ [4]. The lanthanide ion substitutes for yttrium in the YVO_4 lattice [3]. This site has D_{2d} symmetry, which gives rise to a characteristic crystal field splitting of the energy levels and a characteristic intensity pattern of the luminescence lines [5]. When doped with trivalent Eu^{3+} , red-emitting $YVO_4:Eu^{3+}$ phosphor is an encouraging luminescent material with a high color purity, which is caused by the non-centrosymmetric site of Eu^{3+} [6]. The emission spectrum of $YVO_4:Eu^{3+}$ in the visible region is made up of a group of

intense lines at 610.9, 613.6, 615.6 and 619.6 nm, which are all due to transitions from the 5D_0 excited level to the four crystal field components of 7F_2 [5].

Higher photoluminescence (PL) intensities can be achieved by forming solid solution, $Y_{1-x}Gd_xVO_4$ [7–10]. The atoms in $Y_{1-x}Gd_xVO_4$ occupy as follows: Y and Gd in 4a ($0, 3/4, 1/8$), V in 4b ($0, 1/4, 3/8$) and O in 16 h ($0, y, z$), respectively [11]. Most work on the $(Y_{1-x}Gd_x)_{0.94}Eu_{0.06}VO_4$ has focused on its luminescence properties under an excitation of ≥ 243 nm [7–10]. However, to date, there has been little information on the luminescence properties under vacuum ultraviolet (VUV) irradiation for plasma display panels (PDPs). Therefore, for applying the $(Y_{1-x}Gd_x)_{0.94}Eu_{0.06}VO_4$ phosphors to the PDPs, we synthesized the $(Y_{1-x}Gd_x)_{0.94}Eu_{0.06}VO_4$ ($0 \leq x \leq 1.0$) phosphors by ultrasonic spray pyrolysis and investigated the influence of Gd content on the PL properties under an excitation of 147 nm.

2. Experimental

$(Y_{1-x}Gd_x)_{0.94}Eu_{0.06}VO_4$ ($x = 0, 0.25, 0.5, 0.75$, and 1.0) phosphors were synthesized by the ultrasonic spray pyrolysis. Y_2O_3 (99.99%, High Purity Chemicals), Gd_2O_3 (99.99%, High Purity Chemicals), and NH_4VO_3 (99%, High Purity Chemicals) powders were used as the sources of host materials. Also,

* Corresponding author. Tel.: +82 2 3408 3777; fax: +82 2 3408 3664.

E-mail address: kspark@sejong.ac.kr (K. Park).

Eu_2O_3 (99.99%, High Purity Chemicals) powder was used as activator. First, for each composition, the powders were weighed in specific proportions. Y_2O_3 , Gd_2O_3 , and Eu_2O_3 were separately dissolved by HNO_3 to form the nitrates of Y, Gd, and Eu. Then, the organic additive, which was composed of ethylene glycol (99.5%, Samchun Chemical, 0.5 M) and citric acid (EP, Duksan Pure Chemical, 0.5 M), was added in distilled water. NH_4VO_3 powder was dissolved in a mixture of the nitrates and the organic solutions to prepare polymeric precursor solutions.

An ultrasonic aerosol generator was used to atomize the precursor solutions and the mists produced were carried by air (20 l/min) into a hot furnace (1000 °C). The synthesized powders were annealed at 1100 °C for 4 h in air. The crystal structure of the annealed $(\text{Y}_{1-x}\text{Gd}_x)_{0.94}\text{Eu}_{0.06}\text{VO}_4$ powders was analyzed with an X-ray diffractometer (XRD; Rigaku RINT2000). The morphological characteristics of the phosphors were investigated with a scanning electron microscope (SEM; Hitachi S4700). The PL spectra of the powders were obtained using a spectro-fluorophotometer (PSI) with a D_2 flash lamp. The emission spectra were obtained in the VUV region of 147 nm.

3. Results and discussion

We found that the as-synthesized $(\text{Y}_{1-x}\text{Gd}_x)_{0.94}\text{Eu}_{0.06}\text{VO}_4$ phosphors showed fine powder size as well as smooth and spherical morphology. In addition, the powder characteristics of the annealed $(\text{Y}_{1-x}\text{Gd}_x)_{0.94}\text{Eu}_{0.06}\text{VO}_4$ phosphors were smaller size and less spherical compared to the as-synthesized $(\text{Y}_{1-x}\text{Gd}_x)_{0.94}\text{Eu}_{0.06}\text{VO}_4$ phosphors. For example, the SEM images of the as-synthesized and annealed $(\text{Y}_{0.5}\text{Gd}_{0.5})_{0.94}\text{Eu}_{0.06}\text{VO}_4$ phosphors are shown in Fig. 1(a) and (b), respectively.

The XRD patterns of the vanadate-based $(\text{Y}_{1-x}\text{Gd}_x)_{0.94}\text{Eu}_{0.06}\text{VO}_4$ ($0 \leq x \leq 1.0$) phosphors annealed at 1100 °C are shown in Fig. 2. The $(\text{Y}_{1-x}\text{Gd}_x)_{0.94}\text{Eu}_{0.06}\text{VO}_4$ phosphors were solid solution of the constituent oxides, which crystallized in a tetragonal xenotime structure with a space group of $\text{I}4_1/\text{amd}$ (1 4 1) [12]. The XRD peaks moved toward smaller angles with increasing Gd content, indicating that the lattice parameter increased with an increase in Gd content. This is because the ionic radius of Gd^{3+} (0.94 Å) is larger than that of Y^{3+} (0.89 Å) [13]. The crystallite size of the annealed $(\text{Y}_{1-x}\text{Gd}_x)_{0.94}\text{Eu}_{0.06}\text{VO}_4$ ($0 \leq x \leq 1.0$) phosphors was calculated from the broadening of strong XRD peaks, i.e. (2 0 0), (1 1 2), and (3 1 2), by using the Scherrer's equation. The calculated crystallite sizes ranged from 58 nm to 68 nm. There was no definite dependence of crystallite size on the Gd content.

In order to investigate the PL properties of the $(\text{Y}_{1-x}\text{Gd}_x)_{0.94}\text{Eu}_{0.06}\text{VO}_4$ ($0 \leq x \leq 1.0$) phosphors, they were excited under VUV irradiation and then their emission spectra were obtained. The emission spectra of the $(\text{Y}_{1-x}\text{Gd}_x)_{0.94}\text{Eu}_{0.06}\text{VO}_4$ excited at 147 nm are shown in Fig. 3. The spectra consist of three strong peaks at 594, 615, and 619 nm. These peaks are assigned to the transitions from the excited $^5\text{D}_0$ to $^7\text{F}_j$ ($j = 1$ and 2) levels of the Eu^{3+} activator [14]. The emission of electronic dipole $^5\text{D}_0 \rightarrow ^7\text{F}_2$ transition at 615 nm and 619 nm, which is responsible for red

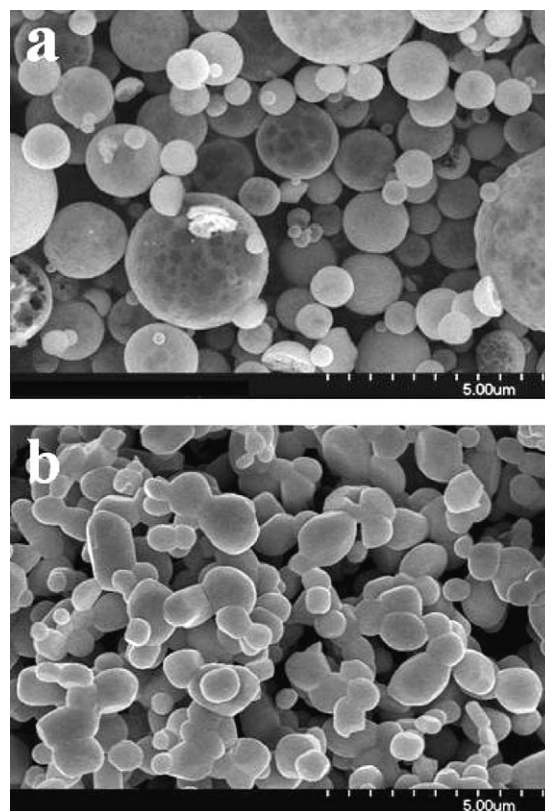


Fig. 1. SEM images of the (a) as-synthesized and (b) annealed $(\text{Y}_{0.5}\text{Gd}_{0.5})_{0.94}\text{Eu}_{0.06}\text{VO}_4$ phosphors.

light emission, is much stronger than that of magnetic $^5\text{D}_0 \rightarrow ^7\text{F}_1$ transition at 594 nm, which is responsible for orange-red light emission. This fact demonstrates that the vanadate-based $(\text{Y}_{1-x}\text{Gd}_x)_{0.94}\text{Eu}_{0.06}\text{VO}_4$ phosphors emit a highly pure red color compared to both borate-based $\text{YBO}_3:\text{Eu}^{3+}$ and $(\text{Y,Gd})\text{BO}_3:\text{Eu}^{3+}$ phosphors. For the latter phosphors, the intensity of the $^5\text{D}_0 \rightarrow ^7\text{F}_2$ transition was much weaker than that of the $^5\text{D}_0 \rightarrow ^7\text{F}_1$ transition, indicating low-purity red color emission [15].

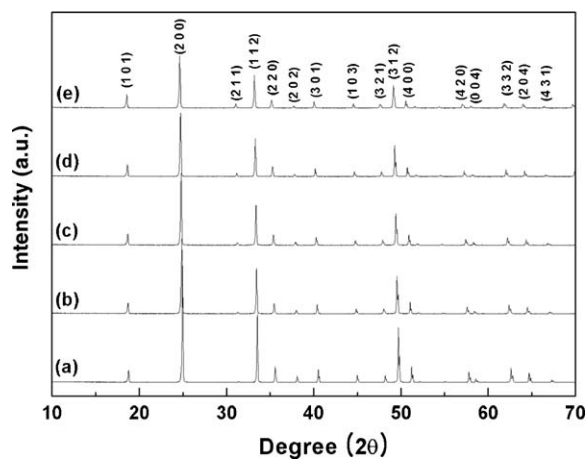


Fig. 2. XRD patterns of the (a) $\text{Y}_{0.94}\text{Eu}_{0.06}\text{VO}_4$, (b) $(\text{Y}_{0.75}\text{Gd}_{0.25})_{0.94}\text{Eu}_{0.06}\text{VO}_4$, (c) $(\text{Y}_{0.5}\text{Gd}_{0.5})_{0.94}\text{Eu}_{0.06}\text{VO}_4$, (d) $(\text{Y}_{0.25}\text{Gd}_{0.75})_{0.94}\text{Eu}_{0.06}\text{VO}_4$, and (e) $\text{Gd}_{0.94}\text{Eu}_{0.06}\text{VO}_4$ phosphors annealed at 1100 °C.

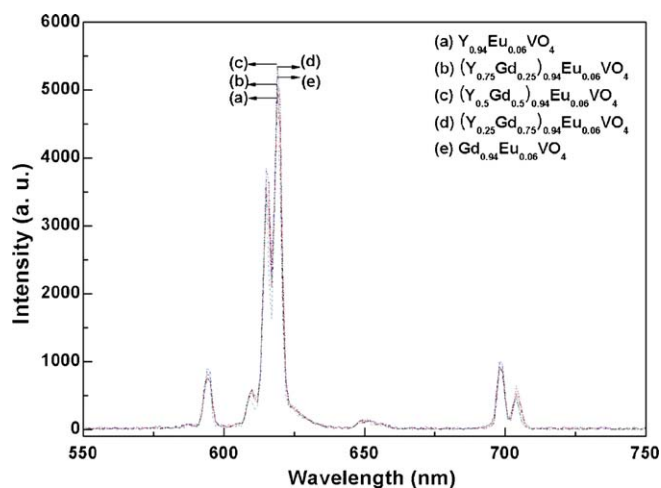


Fig. 3. Emission spectra of the $(Y_{1-x}Gd_x)_{0.94}Eu_{0.06}VO_4$ ($0 \leq x \leq 1.0$) phosphors excited at 147 nm.

Fig. 4 shows the emission intensity of the $(Y_{1-x}Gd_x)_{0.94}Eu_{0.06}VO_4$ at 619 nm as a function of Gd content (x) under VUV excitation. The emission intensity of the $(Y_{1-x}Gd_x)_{0.94}Eu_{0.06}VO_4$ phosphors increased with increasing Gd content, reaching a maximum at $x = 0.5$. Then it decreased with a further increase in Gd content. The increase in PL intensity up to $x = 0.5$ may be caused by the fact that the substituted Gd efficiently absorbed the excitation energy and transferred it to the Eu^{3+} activator [16]. For high Gd content ($x \geq 0.75$), the decrease in emission intensity may be due to the fact that the absorbed VUV photon energy was released as a non-radiation transition instead of visible light owing to the energy transfer between activator Eu^{3+} ions [17].

The Commission Internationale de l'Eclairage (CIE) chromaticity coordinates of the $(Y_{1-x}Gd_x)_{0.94}Eu_{0.06}VO_4$ phosphors are given in Table 1. The values of the x and y coordinates are 0.652–0.658 and 0.324–0.326, respectively, indicating red color emission. The $(Y_{0.5}Gd_{0.5})_{0.94}Eu_{0.06}VO_4$ phosphor emits the purest red color and its coordinate (x, y) is

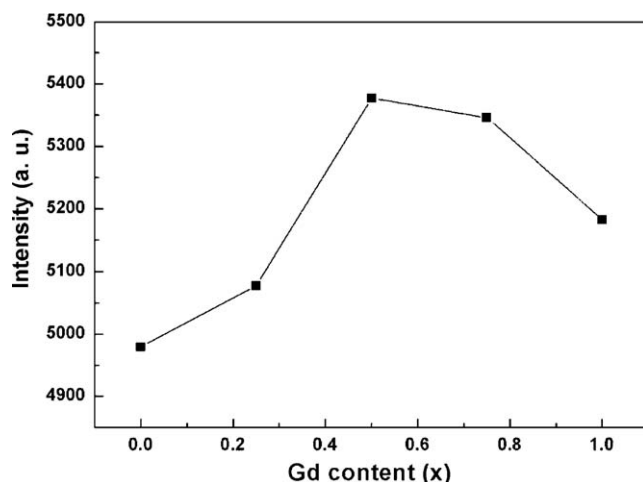


Fig. 4. Emission intensity of the $(Y_{1-x}Gd_x)_{0.94}Eu_{0.06}VO_4$ ($0 \leq x \leq 1.0$) at 619 nm as a function of Gd content (x) under VUV excitation.

Table 1

CIE coordinate of the $(Y_{1-x}Gd_x)_{0.94}Eu_{0.06}VO_4$ ($0 \leq x \leq 1$) phosphors annealed at 1100 °C.

| Sample | CIE coordinates (x, y) |
|---|----------------------------|
| $Y_{0.94}Eu_{0.06}VO_4$ | 0.652, 0.324 |
| $(Y_{0.75}Gd_{0.25})_{0.94}Eu_{0.06}VO_4$ | 0.654, 0.323 |
| $(Y_{0.5}Gd_{0.5})_{0.94}Eu_{0.06}VO_4$ | 0.658, 0.325 |
| $(Y_{0.25}Gd_{0.75})_{0.94}Eu_{0.06}VO_4$ | 0.656, 0.326 |
| $Gd_{0.94}Eu_{0.06}VO_4$ | 0.655, 0.324 |

(0.658, 0.325). The red color purity obtained here is much purer compared to conventional borate-based $YBO_3:Eu^{3+}$ and $(Y,Gd)BO_3:Eu^{3+}$ phosphors. For the borate-based phosphors, the intensity of the magnetic transition was much stronger than that of the electric dipole transition, indicating low-purity red color emission [18]. For example, the CIE coordinate (x, y) of $Y_{0.9}Eu_{0.1}BO_3$ phosphor was (0.505, 0.337) [19].

4. Conclusions

The $(Y_{1-x}Gd_x)_{0.94}Eu_{0.06}VO_4$ phosphors were solid solution of the constituent oxides, which crystallized in a tetragonal xenotime structure with a space group of $I4_1/amd$ (1 4 1). In spite of the annealing, the powders maintained the size and morphology of the as-synthesized powders. Higher Gd content yielded higher lattice parameter. The calculated crystallite sizes ranged from 58 to 68 nm and had no definite dependence of crystallite size on the Gd content. The $(Y_{1-x}Gd_x)_{0.94}Eu_{0.06}VO_4$ phosphors emitted a highly pure red color compared to the borate-based phosphors. The emission intensity of the $(Y_{1-x}Gd_x)_{0.94}Eu_{0.06}VO_4$ phosphors increased with increasing Gd content up to $x = 0.5$. We believe that the partial incorporation of Gd for Y in $Y_{0.94}Eu_{0.06}VO_4$ is highly effective for enhancing PL properties.

References

- [1] L. Tian, S. Mho, Enhanced photoluminescence of $YVO_4:Eu^{3+}$ by codoping the Sr^{2+} , Ba^{2+} or Pb^{2+} ion, J. Lumin. 122–123 (2007) 99–103.
- [2] K.S. Sohn, W. Zeon, H. Chang, S.K. Lee, H.D. Park, Combinatorial search for new red phosphors of high efficiency at VUV excitation based on the YVO_4 ($R = As, Nb, P, V$) system, Chem. Mater. 14 (2002) 2140–2148.
- [3] K. Riwotzki, M. Haase, Wet-chemical synthesis of doped colloidal nanoparticles: $YVO_4:Ln$ ($Ln = Eu, Sm, Dy$), J. Phys. Chem. B 102 (1998) 10129–10135.
- [4] H. Fuess, A. Kallel, Refinement of the crystal structure of some rare earth vanadates RVO_4 ($R = Dy, Tb, Ho, Yb$), J. Solid State Chem. 5 (1972) 11–14.
- [5] S. Erdei, L. Kovács, M. Martini, F. Meinardi, F.W. Ainger, W.B. White, High temperature 3-D thermoluminescence spectra of Eu^{3+} activated YVO_4 – YPO_4 powder systems reacted by hydrolyzed colloid reaction (HCR) technique, J. Lumin. 68 (1996) 27–34.
- [6] Y. Wang, Y. Zuo, H. Gao, Luminescence properties of nanocrystalline $YVO_4:Eu^{3+}$ under UV and VUV excitation, Mater. Res. Bull. 41 (2006) 2147–2153.
- [7] X. Su, B. Yan, H. Huang, In situ co-precipitation synthesis and luminescence of $GdVO_4:Eu^{3+}$ and $Y_xGd_{1-x}VO_4:Eu^{3+}$ microcrystalline phosphors derived from the assembly of hybrid precursors, J. Alloys Compd. 399 (2005) 251–255.

- [8] J. Wu, B. Yan, Photoluminescence intensity of $Y_xGd_{1-x}VO_4:Eu^{3+}$ dependence on hydrothermal synthesis time and variable ratio of Y/Gd, *J. Alloys Compd.* 455 (2008) 485–488.
- [9] T. Minami, T. Miyata, Y. Suzuki, Y. Mochizuki, Accurate calibration and optimized measurement: use of an achromatic compensator in rotating polarizer spectroscopic ellipsometry, *Thin Solid Films* 469–470 (2004) 61–65.
- [10] K.S. Shim, H.K. Yang, B.K. Moon, J.H. Jeong, S.S. Yi, K.H. Kim, Improved photoluminescence of pulsed-laser-ablated $Y_{1-x}Gd_xVO_4:Eu^{3+}$ thin film phosphors by Gd substitution, *Appl. Phys. A* 88 (2007) 623–626.
- [11] J. Isasi, M.L. Veiga, Y. Laureiro, R. Saez-Puche, C. Pico, Synthesis, structural determination and magnetic behaviour of $Y_xGd_{1-x}VO_4$ phases ($x = 0.25, 0.50, 0.75$), *J. Alloys Compd.* 177 (1991) 143–147.
- [12] JCPDS file No. 85-2317.
- [13] W.D. Kingery, H.K. Bowen, D.R. Uhlmann, *Introduction to Ceramics*, 2nd ed., John Wiley and Sons, New York, 1976.
- [14] D. Boyer, G. Bertrand, R. Mahiou, A spectroscopic study of the vaterite form $YBO_3:Eu^{3+}$ processed by sol–gel technique, *J. Lumin.* 104 (2003) 229–237.
- [15] K. Park, J.H. Lee, Y. Kwon, The effect of simultaneous addition of Gd and Al on the photoluminescence characteristics of $(Y_{0.94-x-y}Al_xGd_yEu_{0.06})BO_3$ phosphors, *Mater. Res. Bull.* 44 (5) (2009) 1077–1080.
- [16] B.N. Mahalley, S.J. Dhoble, R.B. Pode, G. Alexander, Photoluminescence in $GdVO_4:Bi^{3+}, Eu^{3+}$ red phosphor, *Appl. Phys. A* 70 (2000) 39–45.
- [17] D.L. Dexter, A theory of sensitized luminescence in solids, *J. Chem. Phys.* 21 (1953) 836–850.
- [18] G. Pan, H. Song, L. Yu, Z. Liu, X. Bai, Y. Lei, L. Fan, Luminescent properties of $YBO_3:Eu^{3+}$ nanosheets and microstructural materials consisting of nanounits, *J. Lumin.* 122–123 (2007) 882–885.
- [19] C. Lin, D. Kong, X. Liu, H. Wang, M. Yu, J. Lin, Monodisperse and core–shell-structured $SiO_2@YBO_3:Eu^{3+}$ spherical particles: synthesis and characterization, *Inorg. Chem.* 46 (2007) 2674–2681.